SHRINKING OF CLUSTER ELLIPTICALS: A TIDAL STRIPPING EXPLANATION AND IMPLICATIONS FOR THE INTRACLUSTER LIGHT

Eduardo S. Cypriano
Southern Astrophysics Research Telescope, Casilla 603, La Serena, Chile; and Laboratório Nacional de Astrofísica, CP 21, 37500-000 Itajubá-MG, Brazil; ecypriano@ctio.noao.edu

Laerte Sodré, Jr.
Departamento de Astronomia, Instituto de Astronomia, Geofísica e Ciências Atmosféricas da Universidade de São Paulo, Rua do Matão 1226, Cidade Universitária, 05508-090 São Paulo, Brazil; laerte@astro.iag.usp.br

Luis E. Campusano[1]
Observatorio Astronómico Cerro Calán, Departamento de Astronomía, Universidad de Chile, Casilla 36-D, Santiago, Chile; luis@das.uchile.cl

Daniel A. Dale[1]
Department of Physics and Astronomy, University of Wyoming, Laramie, WY 82071; ddad@uwyo.edu

and

Eduardo Hardy[1,2]
National Radio Astronomy Observatory, Casilla El Golf 16-10, Santiago, Chile; ehardy@nrao.edu

ABSTRACT

We look for evidence of tidal stripping in elliptical galaxies through the analysis of homogeneous CCD data corresponding to a sample of 228 elliptical galaxies belonging to 24 clusters of galaxies at $0.015 < z < 0.080$. We investigate departures from the standard magnitude–isophotal size relation as a function of environmental (clustercentric distance, local galaxy density) and structural (cluster velocity dispersion, Bautz-Morgan type) properties. We find that, for any particular galaxy luminosity, the elliptical galaxies in the inner and denser regions of the clusters are about 5% smaller than those in the outer regions, which is in good agreement with the finding of Strom and Strom based on photographic photometry. The null hypothesis (i.e., galaxy sizes are independent of the clustercentric distance or density) is rejected at a significance level of better than 99.7%. The numerical models of Aguilar and White predict that tidal stripping can lead to changes in the whole structure of elliptical galaxies, producing shrinkage and brightening of the galaxy qualitatively consistent with our measurements and also with the findings of Trujillo and coworkers that more centrally concentrated elliptical galaxies populate denser regions. Our observational results can be interpreted as evidence for the stripping of stars from elliptical galaxies in the central/denser regions of clusters, contributing to the intracluster light observed in these structures.

Key words: galaxies: clusters: general — galaxies: clusters: individual (A3558) — galaxies: interactions — galaxies: photometry

1. INTRODUCTION

The existence of diffuse optical light in the central region of galaxy clusters is well known (Zwicky 1951; de Vaucouleurs 1960), but its very low surface brightness precluded quantitative analysis. More recently, due to advances in observational and data reduction techniques, accurate measurements of the total amount of this light and its color and spatial distribution became feasible for rich clusters (Uson et al. 1991; Scheick & Kuhn 1994; Gonzalez et al. 2000, 2005; Feldmeier et al. 2002, 2004a). Moreover, single objects, such as planetary nebulae, red giant stars, or supernovae, have been detected in the intracluster medium (ICM; Theuns & Warren 1997; Arnaboldi et al. 1996, 2002, 2003; Feldmeier et al. 1998, 2004b; Ferguson et al. 1998; Gal-Yam et al. 2003).

These studies indicate that between ~10% and 20% (or higher) of the total stellar light of the clusters comes from stars in the ICM. These stars have probably been stripped from cluster galaxies after galaxy-galaxy (Gallagher & Ostriker 1972; Richstone 1976) or galaxy-cluster interactions (Merritt 1984). As a galaxy moves through the cluster, it is subject to the gravitational forces of its neighbors, as well as of the cluster as a whole. As a result of the action of these tidal forces, some galaxy stars may be accelerated to velocities larger than the local escape velocity, being removed from the parent galaxy. This process is called "tidal stripping." In some cases the tidal forces may be so strong that the galaxy as a whole is disrupted. Indeed, a significant fraction of galaxy stars may be dispersed in the ICM after disruption of dwarf spheroidal or low surface brightness disk galaxies (e.g., Lopez-Cruz et al. 1997), as suggested by the light plumes observed in clusters such as Centaurus and Coma (Calcáneo-Roldán et al. 2000; Korchagin et al. 2001).

In the present work we investigate whether stars stripped of elliptical galaxies can make a significant contribution to the intracluster light (ICL). There are some hints that point toward this. First, elliptical galaxies are basically found in the central, denser cluster regions, where close encounters between galaxies

[1] Visiting Astronomer at the Cerro Tololo Inter-American Observatory, National Optical Astronomy Observatory, which is operated by the Association of Universities for Research in Astronomy (AURA), Inc., under a cooperative agreement with the National Science Foundation.

[2] The National Radio Astronomy Observatory is a facility of the National Science Foundation operated under cooperative agreement by AURA, Inc.

are very common. Their almost radial orbits (Ramirez & de Souza 1998) lead them to several close approximations to the cluster center, where tidal forces are very strong. The diffuse light is often distributed like a halo around the brightest cluster galaxy (BCG), sometimes extending beyond ~500 kpc. In their study of the surface brightness distribution of BCGs in 24 clusters, Gonzalez et al. (2005) identify a component, independent of the BCG, that is possibly due to intracluster stars and dynamically linked to the cluster as a whole.

The effects of galaxy-galaxy tidal collisions were studied by Aguilar & White (1985, 1986) through the use of the impulsive approximation and *N*-body numerical simulations of close collisions between galaxies with roughly the same mass and with mass distributions consistent with de Vaucouleurs and King profiles. They quantified the mass and energy changes during such collisions and studied the changes of the mass profiles. They found that the $r^{1/4}$ profile is robust, since it is recovered after a collision, although with different parameters. After strong encounters the central surface brightness becomes brighter and the effective and isophotal radii decrease as mass is stripped out. More recently, the high-resolution *N*-body + SPH numerical simulations of rich clusters by Willman et al. (2004) and Murante et al. (2004) indicate that the accumulation of ICL is an ongoing process linked to infall and stripping events and that the stars comprising the ICL are on average older than the stars in cluster galaxies.

Other works have considered the effects of a smooth cluster potential on a galaxy. Using the impulsive approximation (Merritt 1984; Mamon 2000) or high-resolution numerical simulations (Ghigna et al. 1998), it can be shown that cluster galaxies are truncated at the tidal radius:

$$r_{\rm tid} = C\left(\frac{\sigma_g}{\sigma_{\rm cl}}\right) r_p, \qquad (1)$$

where σ_g and $\sigma_{\rm cl}$ are the velocity dispersions of the galaxy and the cluster, respectively, r_p is the radius of maximum approximation between a galaxy and the cluster center, and C is a nondimensional constant that depends of several factors, e.g., galaxy orbits, and is close to unity. This process is often called "tidal truncation."

It is not clear yet what process is more effective in removing stars from cluster galaxies. Tidal truncation is indeed more efficient in removing halo stars, since $r_{\rm tid}$ is larger than the optical radius for the majority of the galaxies. Anyway, as pointed out by Gnedin (1999), mass is not only lost by instantaneous stripping after cluster-galaxy shocks but also by secular tidal heating.

The first observational detection of tidal stripping of stars from elliptical galaxies came from Strom & Strom (1978a, 1978b, 1978c, 1978d) with a sample of 400 elliptical and S0 galaxies located in six different clusters deeply imaged with photographic plates. These authors found that elliptical galaxies in the center of rich clusters have isophotal radii 10%–30% smaller at a given magnitude than elliptical galaxies in poor clusters or in the outskirts of rich ones, estimating that up to ~37% of the luminous mass of the stripped elliptical galaxies has been lost to the ICM.

Despite the great impact of this work, it has been severely criticized, mainly because it was based on photographic photometry (e.g., Dressler 1984). Giuricin et al. (1989) questioned the statistical analysis done by Strom & Strom, and using photoelectric and CCD data of ~160 elliptical galaxies from the sample of Burstein et al. (1987) did not find any dependence of the magnitude-size relation properties of elliptical galaxies on the environment. In this paper we revisit this topic, using CCD data homogeneously collected and reduced.

TABLE 1

Cluster Sample

Name (1)	z[a] (2)	$\sigma_{\rm cl}$[a] (km s^{-1}) (3)	B-M Type (4)	Total Area (deg^2) (5)	Fraction of Area (%) (6)	N (7)
A85.....	0.0555	941	I	0.05	4.8	12
A114.....	0.0582	911	II	0.39	44.8	15
A119.....	0.0449	685	II–III	0.05	5.3	6
A496.....	0.0326	686	I	0.28	16.6	19
A2670.....	0.0766	873	I–II	0.05	11.4	7
A2806.....	0.0265	433	I–II	0.26	34.0	4
A2877.....	0.0251	1026	I	0.45	10.2	7
A2911.....	0.0800	546	I–II	0.32	12.8	2
A3193.....	0.0346	638	I	0.23	21.3	5
A3266.....	0.0586	1131	I–II	0.18	15.0	17
A3376.....	0.0456	641	I	0.10	14.2	8
A3381.....	0.0372	414	I	0.09	39.3	2
A3389.....	0.0259	511	II–III	0.10	5.8	1
A3395.....	0.0496	823	II	0.10	9.9	10
A3407.....	0.0415	504	I	0.13	29.3	3
A3408.....	0.0405	900	I–II	0.20	12.4	4
A3528.....	0.0538	955	II	0.31	26.7	16
A3558.....	0.0473	935	I	0.56	41.4	35
A3571.....	0.0384	969	I	0.05	2.1	6
A3574.....	0.0152	447	I	0.09	2.2	1
A3656.....	0.0195	366	I–II	0.19	15.5	5
A3667.....	0.0549	987	I–II	0.44	33.9	19
A3716.....	0.0454	842	I–II	0.40	33.4	13
A3744.....	0.0386	624	II–III	0.31	37.9	7
A4038.....	0.0302	826	III	0.33	11.3	4

Notes.—Col. (1): Name of the cluster in the Abell catalog (Abell et al. 1989). Col. (2): Redshift. Col. (3): Radial velocity dispersion. Col. (4): Bautz-Morgan type (Bautz & Morgan 1970). Col. (5): Total imaged area. Col. (6): The ratio of the area covered by the imaging over the whole area inside the R_{200} radius. Col. (7): Number of elliptical galaxies in the sample.

[a] We got redshifts and velocity dispersions from the Abell cluster redshift compilation of H. Andernach & E. Tago (2006, in preparation); see Andernach & Tago (1998) for a description.

The layout of the paper is as follows. In § 2 we describe the observational material and the cluster sample and present our method for the extraction of galaxy photometric parameters, as well as the selection criteria of the final galaxy sample. In § 3 we present our results on galaxy sizes, which are discussed in § 4. In § 5 we summarize the main conclusions of this work. Throughout this paper we adopt, when necessary, a ΛCDM cosmology with $H_0 = 70\ h_{70}$ km s^{-1} Mpc^{-1}, $\Omega_M = 0.3$, and $\Omega_\Lambda = 0.7$.

2. THE DATA

2.1. *The Cluster Sample and the Observations*

The galaxy sample discussed in this work was extracted from the set originally obtained as part of the Ph.D. thesis of D. A. Dale on peculiar motions of clusters with $z < 0.1$ (Dale et al. 1997, 1998, 1999a, 1999b, 1999c). The original cluster sample was selected from nearby ($cz < 18{,}000$ km s^{-1}) objects of the Abell et al. (1989) cluster catalog in order to uniformly cover as much of the whole sky area as possible. Although the cluster selection criteria and imaging characteristics were chosen to optimize the peculiar-motion study, the resulting database is useful for many other studies, since it was homogeneously observed and reduced, has high photometric accuracy, and the cluster sample is representative of the low-redshift cluster population (Cypriano et al. 2001). For the present study, only the southern part of this sample has been used. The clusters and some of their properties that are relevant for this work are presented in Table 1.

The observational material consists of several Kron-Cousins *I*-band images obtained with the 0.9 m Cerro Tololo Inter-American Observatory telescope. The details of the observations are discussed elsewhere (Dale et al. 1997, 1998), and here we only summarize them. The detector used was the 2k × 2k Tek2k No. 3 CCD, with a scale of 0.″4 pixel^{-1}, resulting in a field of 13.′5 × 13.′5 per image. The exposure time was 600 s in all cases. The images reach 23.0–23.8 *I* mag arcsec^{-2} at the 1 σ level over the background, with a median of 23.6 *I* mag arcsec^{-2}. The median seeing of the images is 1.″52 and ranges from 1.″16 to 2.″80.

These images, consisting of several pointings per cluster, in general do not uniformly cover a cluster, since they were taken in regions near spiral galaxies, although the central regions of the clusters are always covered. For each cluster, the fraction of the projected area inside the R_{200} radius (see § 2.4) covered by the imaging is also shown in Table 1. The actual distribution of pointings is presented in Dale et al. (1997, 1998, 1999c).

2.2. *Determination of Photometric Parameters*

Most of the images used here were obtained under good photometric conditions. The absolute calibration of the magnitudes was done by using the standard photometric stars of Landolt (1992). The photometric zero-point calibration could be determined with a median accuracy of 0.018 mag, never larger than 0.031 mag.

In this work we have used an isophotal radius as an estimator of the galaxy size because its logarithm is very well correlated with magnitude (Spearman rank correlation coefficient $r_S = -0.99$). On the other hand, the log of the radius that encloses half of a galaxy's light (the effective radius r_e) shows a significantly poorer correlation with magnitude ($r_S = -0.86$). The Petrosian radius (Petrosian 1976) is also less well correlated with magnitude ($r_S = -0.84$), which is not unexpected, since elliptical galaxies spanning a range of 5 absolute magnitudes have different profiles (Caon et al. 1993).

The isophotal quantities are defined at the same isophotal limit in the galaxy rest frame ($\mu_{\rm lim}$). The corresponding isophotal threshold (μ_t) in the observer rest frame is given by the following expression:

$$\mu_t = \mu_{\rm lim} + A_I + 10 \log (1 + z) + k(z), \qquad (2)$$

where A_I is the Galactic absorption in the *I* band, $10 \log (1 + z)$ is the correction due to the cosmological dimming, and $k(z)$ is the *k*-correction.

The values for Galactic absorption adopted here are those given by Schlegel et al. (1998) and range from 0.032 to 0.363 for the clusters in the sample. The *k*-corrections are from Poggianti (1997), assuming her model for elliptical galaxies, and range from 0.006 mag for the nearest cluster (A3574, $z = 0.014$) to 0.035 mag for the farthest one (A2670, $z = 0.076$). The cosmological dimming factor ranges from 0.140 to 0.318 mag. The median value of $\mu_t - \mu_{\rm lim}$ is 0.32 mag.

The surface photometry was performed with the task *ellipse* of IRAF STSDAS.[3] The output of this program is a list of several parameters, such as ellipticity, local intensity, and magnitude, as a function of the semimajor axis value. Using as a radius the geometric average of the semimajor and semiminor axes, the so-called equivalent radius, the isophotal radius ($r_{\rm iso}$) is estimated from the galaxy isophotal brightness profile as the radius corresponding to μ_t, and then the isophotal magnitude ($m_{\rm iso}$) inside $r_{\rm iso}$ is determined. Using the equivalent radius instead of the semimajor axis, we remove possible bias due to different ellipticities between galaxies.

A de Vaucouleurs (1948) and an exponential profile were also fitted to the isophotal brightness profiles. Following the procedure described in Scodeggio et al. (1998), we removed from the fitting an inner region with radius equal to 2 times the FWHM of stellar sources. These fittings were used as part of the selection of elliptical galaxies (see § 3.3).

The medians of the formal errors are 0.02 in magnitude and 3.3% in $r_{\rm iso}$, where errors in $r_{\rm iso}$ have been calculated as

$$\sigma(r_{\rm iso}) = \sigma_\mu \frac{dr}{d\mu}, \qquad (3)$$

with σ_μ being the error of the corresponding surface brightness.

A check of the internal consistency of these errors can be obtained from a sample of 16 galaxies that are present in two different images. The rms differences between isophotal magnitudes and isophotal radii measured in different images are 0.02 and 2.7%, respectively, both in agreement with the formal errors.

2.3. *Sky Subtraction*

Since the sky subtraction is critical in the kind of study presented here, the procedure of sky determination is now explained in detail. First, the software SExtractor (Bertin & Arnouts 1996) is used to determine the average sky value for the entire field. Then the galaxy image is modeled using the IRAF task *ellipse* and removed from a sky-subtracted image. We then estimate the residuals in the local sky by examining the residuals in a square region centered in the subtracted galaxy with a side length equal to at least 2 times the galaxy major axis at μ_t. The size of this region was determined after several tests and proved to be convenient for estimation of the local background. The new local sky level is obtained by removing the mean value of the residuals from the previously adopted background level. Next, the procedure of surface photometry and image subtraction is done again, using this new value for the value of the local sky. The whole process is repeated until no significant local sky variations are found. Generally, two iterations were enough. This process starts with the brightest galaxy in the field and continues in order of increasing magnitude to avoid luminosity contamination of the galaxy by the envelope of the BCG and other bright galaxies in the cluster field.

2.4. *Selection of the Galaxy Sample*

The selection of elliptical galaxies for the analysis was done following several steps. A first selection was done based on the galaxy morphology and the form of its light profile. Initially, all galaxies that are obvious spirals were removed from the sample. Then, by comparing galaxy light profiles with exponential and de Vaucouleurs (1948) profiles, it was possible to remove from the sample of elliptical galaxies some apparently featureless disk-like galaxies.

Next, the morphological classification was checked with previous classifications using the NASA/IPAC Extragalactic Database.[4] Nearly half of the galaxies in the sample had previous classifications. About 30% of them were classified as S0 and removed from the sample. Only a few cases of early-type spirals classified as elliptical galaxies were found. Galaxies with redshifts inconsistent with those of the clusters were also removed.

[3] IRAF is distributed by the National Optical Astronomy Observatory, which is operated by AURA, Inc., under cooperative agreement with the National Science Foundation.

[4] This research has made use of the NASA/IPAC Extragalactic Database, which is operated by the Jet Propulsion Laboratory, California Institute of Technology, under contract with the National Aeronautics and Space Administration.

Due to the presence of a disk component, S0 galaxies tend to have larger sizes at a given magnitude than elliptical galaxies. However, since the radial distributions of S0 and elliptical galaxies in clusters do not strictly match each other, there is the possibility that misclassification of lenticular as elliptical galaxies might produce a radial trend that could bias our results, because the radial distribution of the former is slightly more extended than the latter (Whitmore et al. 1993). This is difficult to evaluate because we do not know a priori either the number of misclassifications or their radial distribution. However, we expect that they would be more common in the inner than the outer parts of the clusters due to the difficulty introduced by the cluster diffuse light in the detection of faint disks. If this is indeed the case, the bias introduced would only dilute the radial trends discussed here.

To ensure a high photometric quality of the data, only galaxies with an isophotal radius larger than 2 times the FWHM of point sources plus 0.″8 (2 pixels) were included in the sample. In addition, images in which the chosen isophotal limit is within 1 σ of the sky brightness were excluded from the analysis. The faintest galaxies of the sample have 17.5 I mag.

Objects with signs of contamination by a nearby object, which could be easily recognized on the light profiles and in the residuals that remain after the subtraction of the galaxy, were also removed from the sample. Objects with strong gradients in the local background, precluding an accurate sky subtraction, were also removed.

As a final criterion, only galaxies with clustercentric distances lower than R_{200} were included in the analysis. This is the radius at which the mass density is $\sim$200 times larger than the critical density and is a good approximation to the virial radius. This radius R_{200} is estimated using the expression (Carlberg et al. 1996)

$$R_{200} = \frac{\sqrt{3}\sigma_{\rm cl}}{10H(z)}, \tag{4}$$

where $\sigma_{\rm cl}$ is the one-dimensional velocity dispersion of the cluster and $H(z)$, a function of the cosmological parameters, is the Hubble factor at the cluster redshift.

The size of the sample depends on the isophotal limit chosen. Using a fiducial isophotal limit in the galaxy rest frame of $\mu_{\rm lim} = 22.75$ I mag arcsec^{-2}, which avoids significant incompleteness, the full sample contains 228 elliptical galaxies, 172 (75%) of them with spectroscopic confirmation of cluster membership. The number of elliptical galaxies per cluster in the final sample is presented in Table 1.

At this point it is important to warn the reader that the galaxy sample selected for this work is not complete in any sense due to the way the fields of the clusters were imaged and also because we have rejected a number of objects for which we were not able to perform the surface photometry properly, mainly because of light contamination by a neighbor. This problem is more severe in the central parts of the clusters, since there the surface density of objects is large. Both factors of incompleteness can change the number of objects as a function of the radius, but it is not expected that they can lead to any bias that can explain the trends identified in this work (see § 3) because they are completely independent of the photometric parameters of the galaxies.

3. RESULTS

3.1. *The Magnitude-Size Relation for Cluster Elliptical Galaxies*

In Figure 1 we plot the observed relationship between the absolute isophotal magnitude and the isophotal radius (at the fiducial isophotal limit in the galaxy rest frame of $\mu_{\rm lim} = 22.75$ I mag arcsec^{-2}), as well as standard least-squares fits of linear and quadratic models.

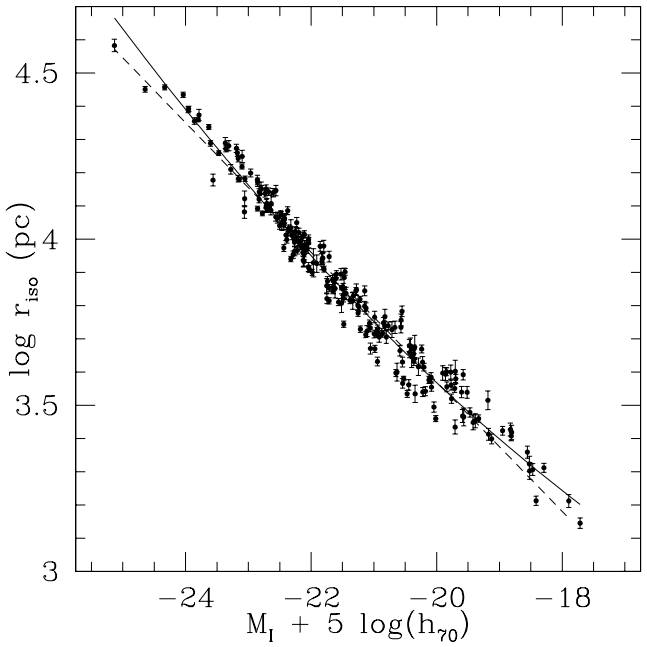

FIG. 1.—Size-magnitude relation in the I band for cluster elliptical galaxies. The isophotal limit at which radii and magnitudes are measured in the galaxy rest frame is $\mu_{\rm lim} = 22.75$ I mag arcsec^{-2}. The dashed and solid lines are the least-squares fit to the data using linear and quadratic models, respectively.

It can be appreciated in this plot that the linear model (*dashed line*) fits the data well but with some systematic residuals in both the faint and bright extremes. However, these residuals are minimized by the use of a quadratic model (*solid line*). Actually, a likelihood ratio test indicates that a quadratic model is significantly more reliable than a linear model. Higher order models do not statistically improve the likelihood of the fit.

Hereafter, $\langle r_{\rm iso}\rangle(M)$ will be used to denote the isophotal radius of a galaxy that, given its I magnitude, obeys the magnitude-size relation represented by the solid line in Figure 1. We define

$$\eta \equiv \frac{r_{\rm iso}}{\langle r_{\rm iso}\rangle(M)}, \tag{5}$$

where $r_{\rm iso}$ is the actual isophotal radius, as a convenient way of measuring the deviation of the isophotal radius of a galaxy from the value that is expected given its luminosity. Note that $\eta < 1$ represents an effective "shrinkage" of a galaxy. The mean uncertainty in η is 0.037, taking into account the error in the measured isophotal radius and in the fitted radius-magnitude relation.

We present in Figure 2 the distribution of η for all galaxies in our sample. Its average value is 1.005 with a standard deviation of 0.10 (or 10%). The observational errors in $r_{\rm iso}$ can account for one-third of this scatter, and the errors on the magnitudes are negligible (formal errors in M_I are typically 0.02 mag). Indeed, most of the variance in η is due to cosmic scatter in the magnitude-size relation.

We verified that the image quality is not affecting η measurements. The Spearman rank correlation coefficient between η and the seeing (FWHM) of the images is 0.1, indicating a nonexistent or very low dependence between these two quantities.

3.2. *Galaxy Sizes as a Function of Clustercentric Distances*

In the 1970s, Strom & Strom claimed that they had found evidence for tidal stripping in galaxy clusters based on an analysis of

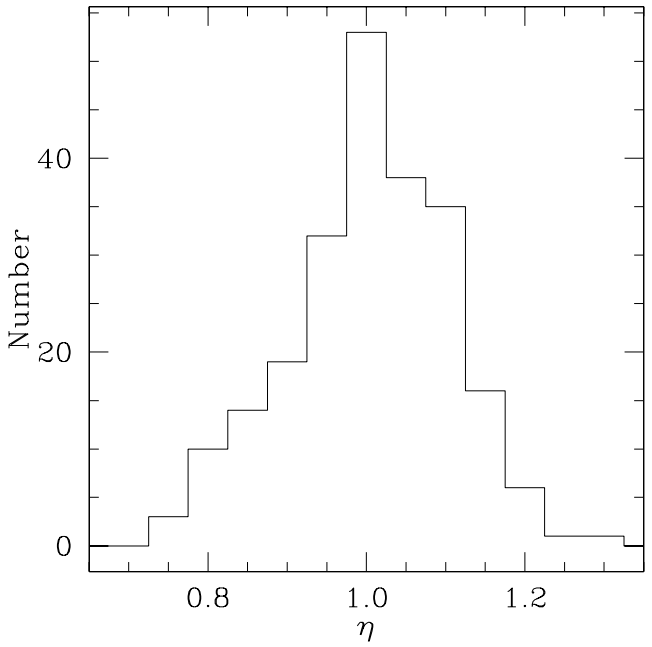

FIG. 2.—Distribution of values of the ratio between the measured isophotal radius of a galaxy and that expected for a galaxy with the same magnitude η for the galaxies of our sample.

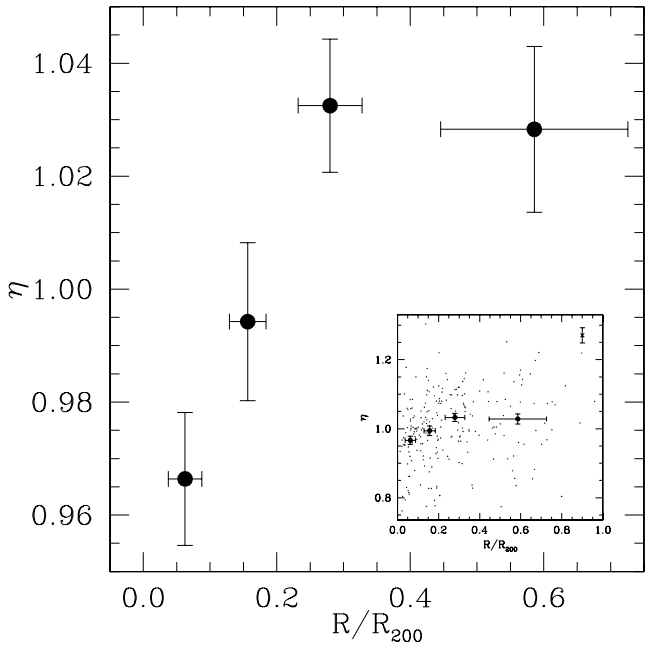

FIG. 3.—Mean value of η as a function of the normalized projected radial distance R/R_{200}. The main plot shows bins with approximately the same number of data points. The horizontal error bars are the 1 σ dispersion of the data, and the vertical ones are the error of the mean ($\sigma/\sqrt{N}$). The inset shows the individual data points. In the upper right corner of the inset is shown an average η error bar.

the isophotal radius of cluster galaxies and a function of its clustercentric radial position (Strom & Strom 1978d). We carry out a similar analysis in this section using the cluster galaxies of our sample.

Since the number of data points per cluster is generally low, we have decided to use an "ensemble " technique, where the data of all clusters are analyzed together. For this, the clustercentric distances of the galaxies R were normalized by the value of R_{200} for the cluster. Figure 3 presents the ratio η as a function of the normalized clustercentric distance R/R_{200} for our sample.

To investigate radial trends in the optical extent of elliptical galaxies, we examine whether η varies with R/R_{200}. Indeed, by dividing the sample with respect to the median of R/R_{200} (0.202), we find that galaxies in the group near the center ($\langle R/R_{200}\rangle = 0.11$) have $\eta = 0.980 \pm 0.009$, whereas those in the outer group ($\langle R/R_{200}\rangle = 0.43$) have $\eta = 1.030 \pm 0.009$. The mean difference in η between the two groups is 5.0% $\pm$ 1.3%, ruling out at a 3.8 σ (99.99%) confidence level (CL) the null hypothesis that sizes are independent of the clustercentric distance.

Comparing the medians, which are more robust estimators of location than the means, galaxies of a given luminosity in the outer group are 5.1% larger than those in the inner regions of the clusters. It is interesting to verify how this result changes as a function of $\mu_{\rm lim}$. In Table 2 we show the difference in η (for medians and means as estimators) of galaxies in these two groups of projected radial distances for different isophotal limits. For both estimators, this difference tends to increase toward fainter values of $\mu_{\rm lim}$, although this gradient is well inside the errors.

The results of a Student's t-test for the statistical significance of the difference of the mean value of η for the two radial groups are also shown in Table 2 and indicate that this difference is significant for all values of $\mu_{\rm lim}$. Note that the difference between the medians is almost always larger than that between the means.

The trend suggested by the data in Table 2 is that the differences in η of the radial groups increases for fainter isophotal limits. This is particularly clear for the difference between medians. A word of caution here is that the significance of this gradient is low due to the errors in these differences. We show in Figure 3 mean values of η for four radial bins with approximately the same number of data points in each one. The figure suggests that η increases monotonically with radius, possibly reaching a plateau at $R/R_{200} \sim 0.4$.

Unfortunately, most of the clusters do not have a sufficiently large number of galaxies in our sample to allow separate analyses. However, Abell 3558 is an exception. This cluster, in the center of the Shapley supercluster, is very rich and has 36 galaxies in our sample, allowing a statistical analysis. The η-radius relation for Abell 3558 is very significant, as shown in Figure 4. The difference between mean values of η below and above $R/R_{200} = 0.202$ (0.68 h_{50}^{-1} Mpc) is 9.8% $\pm$ 3.6%.

In Table 3 we show the difference in η between the inner and the outer radial groups of galaxies for the five clusters that have at least 15 galaxies in our sample. These clusters are among the richest in Table 1. In four of the five clusters the galaxies in the outer group tend to be larger than those in the inner group, although for one of them (A3266) the difference is not really significant. For A3528 the difference is in the opposite direction but, again, the significance is low.

3.3. *Galaxy Sizes as a Function of the Local Galaxy Density*

We are also interested in verifying whether η varies with the local galaxy density. Since our imaging covers the clusters only partially, to avoid incompleteness in the spatial sampling we have used SuperCOSMOS data (Hambly et al. 2001) to obtain a catalog of the galaxies projected onto the cluster fields. We have selected only galaxies brighter than $R = 16.5$.

The local surface density associated with each galaxy in our sample has been computed from the projected distance to its sixth closest SuperCOSMOS neighbor (R_6) using the estimator of Casertano & Hut (1985):

$$\Sigma = \frac{5}{\pi R_6^2}. \qquad (6)$$

TABLE 2

VARIATION OF DIFFERENCES OF η FOR GALAXIES IN THE OUTER AND INNER RADIAL GROUPS AS A FUNCTION OF THE LIMITING ISOPHOTE

				STUDENT'S t–TEST	
μ_{lim} (mag arcsec^{-2})	NUMBER OF GALAXIES	DIFFERENCE BETWEEN MEDIANS (%)	DIFFERENCE BETWEEN MEANS (%)	t	Probability (%)
(1)	(2)	(3)	(4)	(5)	(6)
21.50	151	5.4	4.7 ± 1.1	4.4	100.00
21.75	167	4.9	5.0 ± 1.1	4.5	100.00
22.00	179	6.1	4.8 ± 1.2	4.2	100.00
22.25	191	5.4	4.6 ± 1.3	3.7	99.97
22.50	210	4.8	5.0 ± 1.2	4.0	99.99
22.75	228	5.1	5.0 ± 1.3	3.8	99.98
23.00	200	8.2	7.0 ± 1.6	4.5	100.00

NOTES.—Col. (1): Isophotal limit in the I-band in the galaxy rest frame. Col. (2): Number of galaxies. Col. (3): Differences between the medians. Col. (4): Differences between the means and their errors. Col. (5): Value of t from the Student's t-test. Col. (6): Probability that the observed difference between the two radial groups will not be caused by statistical fluctuations.

This quantity should be corrected for contamination by foreground and background galaxies.

This field contamination was estimated as the median surface density of galaxies in a ring at $4.5R_{200} \pm 0.2R_{200}$ of the cluster center. However, this correction is quite sensitive to the variance of the field galaxy counts often produced by large-scale structures near the cluster or in its line of sight. The cluster A3558, in the center of the Shapley supercluster, illustrates this problem well. Despite its richness (Abell richness class 4), the densities estimated here are among the lowest of the whole sample because the background counts are strongly enhanced due to the presence of several clusters in the region. For this reason, we also analyzed the data without any background subtraction.

Figure 5 shows the relation between η and the logarithm of the corrected projected number density. The figure suggests that there is a tendency for η to decrease with increasing surface density.

The difference in η between galaxies in environments with densities larger and smaller than the median for the background subtracted sample is 3.1% (median) and 3.3% ± 1.3% (mean; 98.6% CL). The values for the non-background-subtracted densities are similar: 3.3% (median) and 4.0% ± 1.3% (mean; 99.7% CL). The median value of Σ for the background-subtracted sample is 51.3 Mpc^{-2}; it is 84.3 Mpc^{-2} for the non-background-subtracted sample.

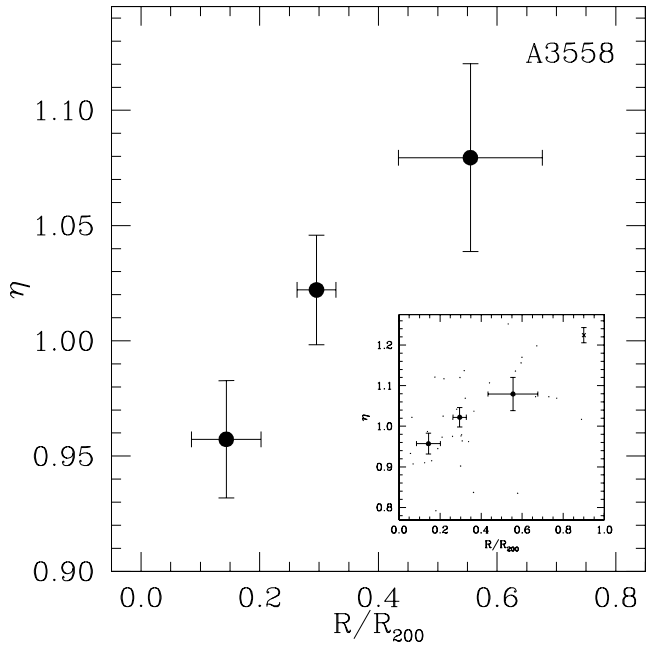

FIG. 4.—Distribution η as a function of the normalized projected radial distance R/R_{200} for galaxies in Abell 3558.

3.4. *Galaxy Sizes as a Function of Cluster Properties*

In order to understand the origin of the stripping mechanism it is important to verify whether and how the isophotal diameters of the galaxies depend on cluster properties. Here we analyze two of them: velocity dispersion and Bautz-Morgan type, which, in principle, are approximately related to mass and evolutionary phase, respectively. In Figures 6 and 7 we show the dependence of η as a function of these parameters.

At first glance neither of these figures displays a clear correlation, as those found for the clustercentric distance and the local density. In Figure 6 it can be seen that galaxies in clusters in the smallest velocity dispersion bin present values of η significantly smaller than those in the other clusters.

Figure 7 shows how η varies with the morphological type of the clusters. Again, we cannot see any trend here. What is noteworthy in this figure, however, is that elliptical galaxies (excluding the BCG) in the inner region of cD clusters (Bautz-Morgan type I) tend to be smaller than those in other cluster types, especially those closest to the cluster center. Actually, the inner galaxies of B-M type I clusters are the smallest in the present sample. A similar result was obtained by Sandage & Hardy (1973), who found that elliptical and lenticular galaxies in type I clusters are dimmer, at a given radius, than in type II clusters.

TABLE 3

VARIATION OF DIFFERENCES OF η FOR GALAXIES IN THE OUTER AND INNER RADIAL GROUPS FOR INDIVIDUAL CLUSTERS

				STUDENT'S t-TEST	
CLUSTER	NUMBER OF GALAXIES	DIFFERENCE BETWEEN MEDIANS (%)	DIFFERENCE BETWEEN MEANS (%)	t	Probability (%)
A3558.....	35	13.6	9.8 ± 3.6	2.5	98.3
A3667.....	19	11.1	10.2 ± 3.8	3.0	99.3
A496.....	19	14.4	15.7 ± 4.6	3.5	99.7
A3266.....	17	1.9	1.6 ± 2.9	0.5	36.0
A3528.....	16	−9.7	−6.9 ± 6.3	−1.2	−75.2

NOTE.—Only clusters with more than 15 galaxies in the sample.

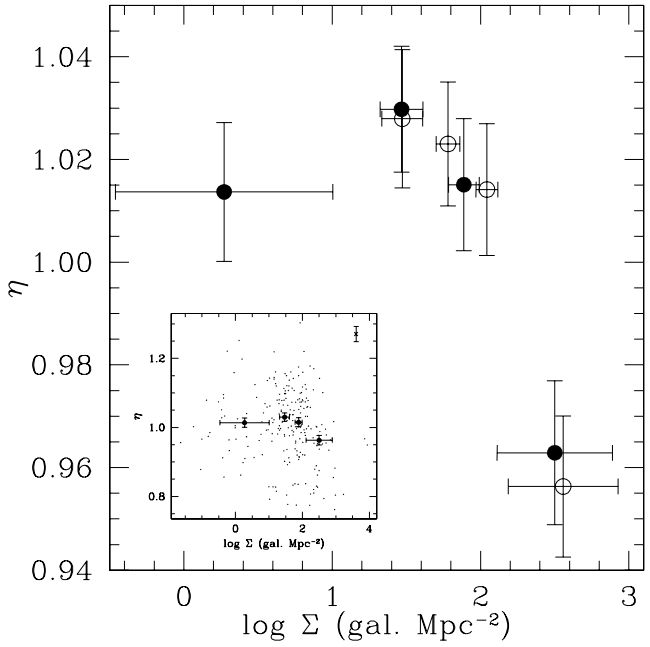

FIG. 5.—Distribution of η as a function of the logarithm of the projected number density of galaxies Σ. The filled circles show averages of bins with similar numbers of data points for the background-subtracted values of the density. The open circles correspond to the non-background-subtracted densities. The horizontal error bars are the 1 σ dispersion of the densities in each bin, and the vertical ones are the errors of the means. In this plot negative densities are represented as the logarithm of the absolute density value times -1.

3.5. *Is There a Dependence of η with Magnitude?*

An important check is to verify whether the effects found here are an artifact of the fitted magnitude-size relation or the result of luminosity segregation. We address this issue in Figure 8.

Figure 8 (*left*), presenting the luminosity distribution as a function of the clustercentric radius, shows a hint that the brighter

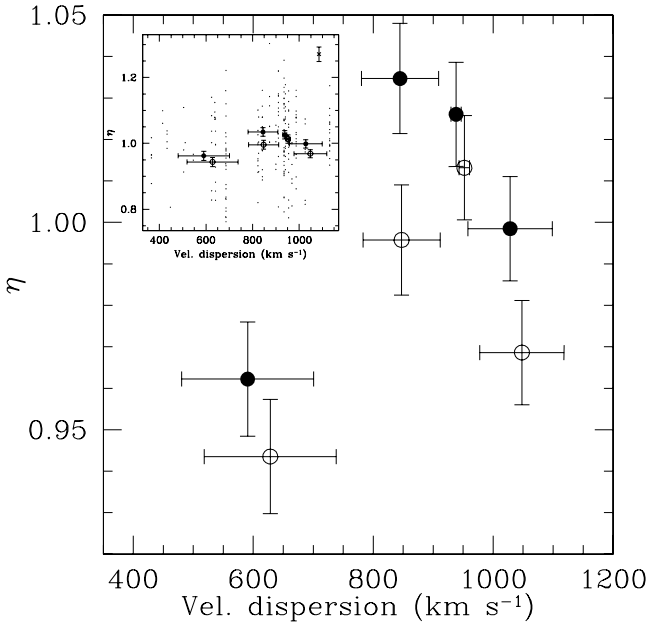

FIG. 6.—Distribution of η as a function of the dispersion of velocity of the cluster. The circles represent the mean value of η with its error in the mean; the horizontal bars represent the interval of σ_{cl} associated with each bin. Filled circles represent mean values for all galaxies in the bin, whereas the open circles contain only galaxies with clustercentric distances less than $0.202R_{200}$. For clarity, we shifted the open circles horizontally by 20 km s^{-1}.

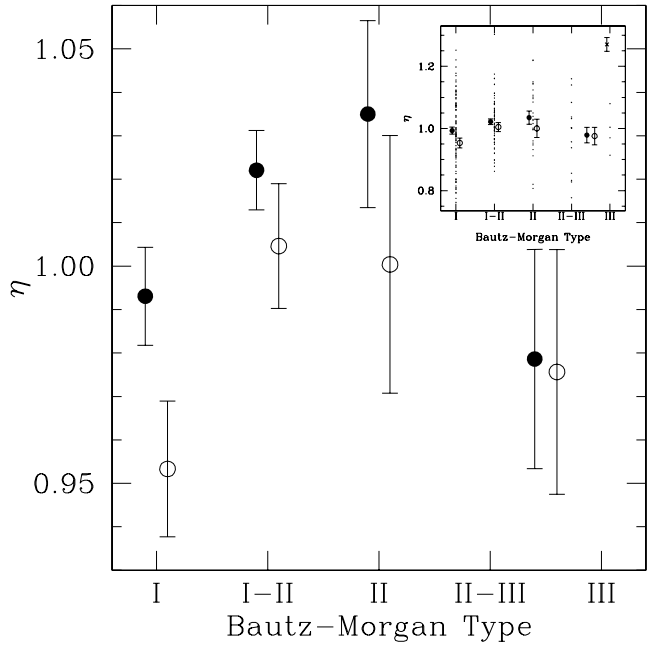

FIG. 7.—Same as Fig. 6, but as a function of the Bautz-Morgan type.

galaxies tend to be found in the outer regions. The difference considering only two radial bins, however, is rather insignificant, 0.27 ± 0.18 mag. Moreover, Figure 8 (*right*) reveals that there is not a monotonic dependence between magnitude and η. For instance, there is no significant relative size difference between the bright and faint half of the sample, $0.8\% \pm 1.4\%$. In fact, this plot shows a difference between η values at the extremes and the center of the magnitude distribution. An inspection of Figure 1 shows that this is produced by the residuals of the fit of the magnitude-size relation with our quadratic model. Rather than indicating segregation (or antisegregation), the trends in Figure 8 probably reflect features of the galaxy sample, which is not complete in any sense (see § 2).

For a double check, we repeated our analysis considering only galaxies with magnitudes between -23.5 and -20.5. Within this interval, the linear and quadratic fits to the magnitude-size relation are nearly identical. We obtained essentially the same results by doing that, although they are noisier due to the smaller number of data points. We thus conclude that all the results found in this work regarding the relative size of elliptical galaxies in clusters are not artifacts of the magnitude-size relation fit or a function of the galaxy luminosity.

4. DISCUSSION

4.1. *Comparison with Previous Work*

Our main result, the shrinkage of galaxies inhabiting the inner parts of the clusters, is in qualitative agreement with the results of Strom & Strom (1978d). These authors found shrinkage factors of 10%–30% in images reaching isophotal levels as faint as 26 R mag arcsec^{-2}, or $\sim$25.3 I mag arcsec^{-2}, assuming $R - I = 0.7$, which is typical of elliptical galaxies at $z \sim 0$ (Fukugita et al. 1995). This is nearly 2.5 mag arcsec^{-2} fainter than our fiducial isophotal limit, 22.75 I mag arcsec^{-2}, precluding a quantitative comparison between our results in Table 2 and those of Strom & Strom (1978d), because the reduction of the isophotal radius may depend on the isophotal level.

Giuricin et al. (1989) have not found any environmental dependency on the sizes of elliptical galaxies in their sample. Their

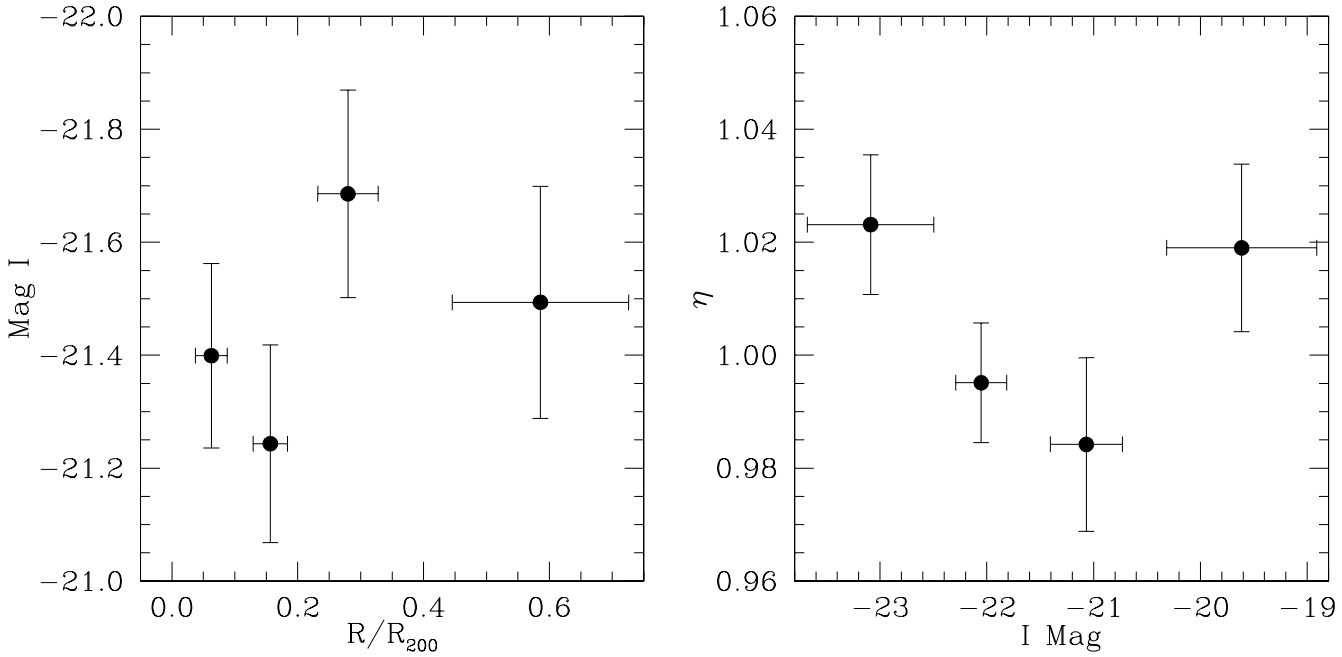

FIG. 8.—*Left*: Mean value of the magnitude as a function of clustercentric distance. *Right*: Mean value of η as a function of the magnitude. In both panels, the bins represent approximately the same number of data points. The horizontal error bars are the 1 σ dispersion of the data, and the vertical ones are the errors of the mean ($\sigma/\sqrt{N}$).

photometry reaches 25.0 B mag arcsec^{-2}, which is roughly as deep as our fiducial value for $\mu_{\rm lim}$ (assuming $B-I\approx 2.27$ for elliptical galaxies; Fukugita et al. 1995). However, they warned in their conclusions that a shrinkage of the isophotal radii of a few percent is consistent with their results, given their observational uncertainties. Actually, Giuricin et al. (1989) report that their typical rms errors in $\log r_{\rm iso}$ are around 0.04 (or 9.6%), and in the best cases (CCD data) they are between 0.02 and 0.03 (4.7%–7.2%), well above the rms error of the log of the isophotal radius in this work, which is 0.015 (3.5%), as explained in § 2. In addition, the present work uses the ensemble technique, which allows us to put together data from different clusters, while Giuricin et al. (1989) divided their sample in subsamples with a small number of data points, leading to results with smaller statistical significance.

Trujillo et al. (2002) have found a related result through the analysis of light concentration for the Virgo and Coma Clusters, indicating that more centrally concentrated elliptical galaxies tend to inhabit the denser regions of galaxy clusters, which is in agreement with the results presented here. When interpreting their results, these authors suggest that the origin of such an effect would be galaxy mergers rather than tidal encounters because, according to Strom & Strom (1978d), the latter would affect only the stars in the outer halo, leaving the cores untouched. However, the numerical simulations of Aguilar & White (1986) convincingly demonstrate (see Fig. 2 of their paper) that tidal shocks do lead to changes in the whole galaxy structure, not just in the outer parts: "...strong collisions produce a shrinkage in r_e and a brightening of μ_e, whereas weak collisions have the opposite effect." Here r_e and μ_e are the parameters of the de Vaucouleurs profile, the effective radius and the surface brightness inside r_e.

Although tidal stripping may not be the only mechanism causing the observed shrinkage of elliptical galaxies, this same mechanism has been validated through numerical simulations (Willman et al. 2004; Richstone 1976) to explain the observed ICL in clusters of galaxies. One of the findings of our work, that for cD clusters (B-M type I) the shrinkage of the central elliptical galaxies is more pronounced than in the other cluster types, is consistent with the early Richstone (1976) claim that cD halos can be formed by stars stripped out from cluster galaxies by tidal shocks, also in agreement with the very recent work of Gonzalez et al. (2005).

4.2. *Tidal Stripping Mechanism*

Finally, we discuss how can it be decided observationally whether tidal truncation (cluster-galaxy collisions) or collisional stripping (galaxy-galaxy encounters) is the dominant mechanism for the shrinkage of the elliptical galaxies. A way to distinguish between these alternatives is by examining how the stripping efficiency (and thus the shrinking of a galactic radius) depends on the cluster velocity dispersion. In the first case, as shown in equation (1), the efficiency should be proportional to $\sigma_{\rm cl}$, because the tidal radius depends on $\sigma_{\rm cl}^{-1}$; in the second case, the dependency should be the opposite, since a lower velocity dispersion leaves room for longer lived, and hence stronger, galaxy-galaxy shocks. Such a test applied to our present data (§ 3.4) unfortunately does not show a clear correlation between galactic size and $\sigma_{\rm cl}$. An analysis of a much larger sample, preferably with deeper data, is necessary to determine which is the dominant mechanism producing the tidal stripping of elliptical galaxies in clusters of galaxies.

5. CONCLUSIONS

We have analyzed a sample of 228 elliptical galaxies belonging to 24 clusters to look for evidence of tidal stripping and to put constraints on the mechanisms behind star removal in cluster galaxies. The stripping was quantified by examining departures of the magnitude–isophotal radius relation for cluster elliptical galaxies, measured by the parameter η, the ratio between the measured isophotal radius of a galaxy (at 22.75 I mag arcsec^{-2} in the galaxy rest frame) and the isophotal radius expected for a galaxy with the same magnitude.

Our main conclusion is that cluster elliptical galaxies of a given magnitude in inner/denser cluster regions are smaller than those in the outer regions by a factor of the order of 5%. The shrinkage factor tends to decrease with increasing distance from the center of the cluster and with decreasing galaxy number density. Although the amount of galaxy stellar mass lost to the ICM remains unknown, it is probably of the order of a few percent of the parent galaxy mass within the optical radius. Thus, it is highly probable that the stars lost by the central cluster elliptical galaxies are significant contributors to the diffuse light observed in clusters of galaxies.

We would like acknowledge Gastão Lima Neto, Gary Mamon, and Claudia Mendes de Oliveira for useful discussions and Nick Suntzeff for encouragement. E. S. C. acknowledges the hospitality of the Department of Astronomy of the Instituto de Astronomia, Geofísica e Ciências Atmosféricas, Universidade de São Paulo, where most of this work was done. The outstanding support at Cerro Tololo Inter-American Observatory is gratefully recognized. E. S. C. (CNPq, Brazil, fellow) and L. S. acknowledge support by the Brazilian agencies FAPESP and CNPq. L. E. C. was partially funded by Fondecyt (Chile) grant 1040499.

REFERENCES

Abell, G. O., Corwin, H. G., Jr., & Olowin, R. P. 1989, ApJS, 70, 1
Aguilar, L. A., & White, S. D. M. 1985, ApJ, 295, 374
———. 1986, ApJ, 307, 97
Andernach, H., & Tago, E. 1998, in Current Status of the ACO Cluster Redshift Compilation, ed. V. Müller et al. (Singapore: World Scientific), 147
Arnaboldi, M., et al. 1996, ApJ, 472, 145
———. 2002, AJ, 123, 760
———. 2003, AJ, 125, 514
Bautz, L. P., & Morgan, W. W. 1970, ApJ, 162, L149
Bertin, E., & Arnouts, S. 1996, A&AS, 117, 393
Burstein, D., Davies, R. L., Dressler, A., Faber, S. M., Stone, R. P. S., Lynden-Bell, D., Terlevich, R. J., & Wegner, G., 1987, ApJS, 64, 601
Calcáneo-Roldán, C., Moore, B., Bland-Hawthorn, J., Malin, D., & Sadler, E. M. 2000, MNRAS, 314, 324
Caon N., Capaccioli M., & D'Onofrio M. 1993, MNRAS, 265, 1013
Carlberg, R., Yee, H. K. C., Ellingson, E., Abraham, R., Gravel, P., Morris, S., & Prichet, C. J. 1996, ApJ, 462, 32
Casertano, S., & Hut, P. 1985, ApJ, 298, 80
Cypriano, E. S., Sodré, L., Jr., Campusano, L. E., Kneib, J.-P., Giovanelli, R., Haynes, M. P., Dale, D. A., & Hardy, E. 2001, AJ, 121, 10
Dale, D. A., Giovanelli, R., Haynes, M. P., Campusano, L. E., & Hardy, E. 1999a, AJ, 118, 1489
Dale, D. A., Giovanelli, R., Haynes, M. P., Hardy, E., Campusano, L. E., Hardy, E., & Borgani, S. 1999b, ApJ, 510, L11
———. 1999c, AJ, 118, 1468
Dale, D. A., Giovanelli, R., Haynes, M. P., Scodeggio, M., Hardy, E., & Campusano, L. E. 1997, AJ, 114, 455
———. 1998, AJ, 115, 418
de Vaucouleurs, G. 1948, Ann. d'Astrophys., 11, 247
———. 1960, ApJ, 131, 585
Dressler, A. 1984, ARA&A, 22, 185
Feldmeier, J. J., Ciardullo, R., & Jacoby, G. 1998, ApJ, 503, 109
Feldmeier, J. J., Ciardullo, R., Jacoby, G. H., & Durrell, P. R. 2004, ApJ, 615, 196
Feldmeier, J. J., Mihos, J. C., Morrison, H. L., Harding, P., Kaib, N., & Dubinski, J. 2004, ApJ, 609, 617
Feldmeier, J. J., Mihos, J. C., Morrison, H. L., Rodney, S. A., & Harding, P. 2002, ApJ, 575, 779
Ferguson, H. C., Tanvir, N. R., & Von Hippel, T. 1998, Nature, 391, 461
Fukugita, M., Shimasaku, K., & Ichikawa, T. 1995, PASP, 107, 945
Gallagher, J. S., III, & Ostriker, J. P. 1972, AJ, 77, 288
Gal-Yam, A., Maoz, D., Guhathakurta, P., & Filippenko, A. V. 2003, AJ, 125, 1087
Ghigna, S., Moore, B., Governato, F., George, L., Quinn, T., & Stadel, J. 1998, MNRAS, 300, 146
Giuricin, G., Mardirossian, M., Mezzetti, M., & Pisani, A. 1989, ApJ, 345, 101
Gnedin, O. Y. 1999, Ph.D. thesis, Princeton Univ.
Gonzalez, A. H., Zabludoff, A. I., & Zaritsky, D. 2005, ApJ, 618, 195
Gonzalez, A. H., Zabludoff, A. I., Zaritsky, D., & Dalcanton, J. J. 2000, ApJ, 536, 561
Hambly, N. C., Irwin, M. J., & MacGillivray, H. T. 2001, MNRAS, 326, 1295
Korchagin, V., Tsuchiya, T., & Miyama, S. M. 2001, ApJ, 549, 244
Landolt, A. U. 1992, AJ, 104, 340
Lopez-Cruz, O., Yee, H. K. C., Brown, J. P., Jones, C., & Forman, W. 1997, ApJ, 475, L97
Mamon, G. A. 2000, in ASP Conf. Ser. 197, Dynamics of Galaxies: From the Early Universe to the Present, ed. F. Combes, G. A. Mamon, & V. Charmandaris (San Francisco: ASP), 377
Merritt, D. 1984, ApJ, 276, 26
Murante, G., et al. 2004, ApJ, 607, L83
Petrosian, V. 1976, ApJ, 209, L1
Poggianti, B. M. 1997, A&AS, 122, 399
Ramirez, A., & de Souza, R. 1998, ApJ, 496, 693
Richstone, D. O. 1976, ApJ, 204, 642
Sandage, A., & Hardy, E. 1973, ApJ, 183, 743
Scheick, X., & Kuhn, J. R. 1994, ApJ, 423, 566
Schlegel, S., Finkbeiner, D. P., & Davies, M. 1998, ApJ, 500, 525
Scodeggio, M., Giovanelli, R., & Haynes, M. P. 1998, AJ, 116, 2728
Strom, S. E., & Strom, K. M. 1978a, AJ, 83, 73
———. 1978b, AJ, 83, 732
———. 1978c, AJ, 83, 1293
———. 1978d, ApJ, 225, L93
Theuns, T., & Warren, S. J. 1997, MNRAS, 284, L11
Trujillo, I., Aguerri, J. A. L., Gutiérrez, C. M., Caon, N., & Cepa, J. 2002, ApJ, 573, L9
Uson, J. M., Boughn, S. P., & Kuhn, J. R. 1991, ApJ, 369, 46
Whitmore, B. C., Gilmore, D. M., & Jones, C. 1993, ApJ, 407, 489
Willman, B., Governato, F., Wadsley, J., & Quinn, T. 2004, MNRAS, 355, 159
Zwicky, F. 1951, PASP, 63, 61